EPJ manuscript No.
(will be inserted by the editor)

Beta-decay properties of ^{25}Si and ^{26}P

J.-C. Thomas[1,2], L. Achouri[3], J. Äystö[4], R. Béraud[5], B. Blank[1], G. Canchel[1], S. Czajkowski[1], P. Dendooven[6], A. Ensallem[5], J. Giovinazzo[1], N. Guillet[1], J. Honkanen[4], A. Jokinen[4], A. Laird[7], M. Lewitowicz[8], C. Longour[9], F. de Oliveira Santos[8], K. Peräjärvi[10], and M. Stanoiu[11]

[1] Centre d'Etudes Nucléaires de Bordeaux-Gradignan, Allée du Haut-Vigneau, B.P. 120, 33170 Gradignan Cedex, France,
[2] Instituut voor Kern- en Stralingsfysica, Celestijnenlaan 200D, 3001 Leuven, Belgium
[3] LPC Caen, 6 Boulevard du Maréchal Juin, 14050 Caen Cedex, France
[4] Department of Physics, PB 35 (YFL), 40014 University of Jyväskylä, Finland
[5] Institut de Physique Nucléaire de Lyon, 69622 Villerbanne Cedex, France
[6] Kernfysisch Versneller Instituut, Zernikelaan 25, 9747 AA Groningen, Netherlands
[7] Department of Physics and Astronomy, University of Edinburgh, Edinburgh EH9 3JZ, United Kingdom
[8] Grand Accélérateur National d'Ions Lourds, B.P. 5027, 14076 Caen Cedex 5, France
[9] Institut de Recherche Subatomique, 23 rue du Loess, B.P. 28, 67037 Strasbourg Cedex, France
[10] Lawrence Berkeley National Laboratory, 1 Cyclotron Road, Berkeley, CA 94720, USA
[11] Institut de Physique Nucléaire d'Orsay, 15 rue G. Clémenceau, 91406 Orsay Cedex, France

the date of receipt and acceptance should be inserted later

Abstract. The β-decay properties of the neutron-deficient nuclei ^{25}Si and ^{26}P have been investigated at the GANIL/LISE3 facility by means of charged-particle and γ-ray spectroscopy. The decay schemes obtained and the Gamow-Teller strength distributions are compared to shell-model calculations based on the USD interaction. $B(GT)$ values derived from the absolute measurement of the β-decay branching ratios give rise to a quenching factor of the Gamow-Teller strength of 0.6. A precise half-life of $43.7\ (6)\ ms$ was determined for ^{26}P, the $\beta-(2)p$ decay mode of which is described.

PACS. 29.30.Ep Charged-particle spectroscopy – 29.30.Kv X- and gamma-ray spectroscopy – 23.90.+w

1 Introduction

1.1 Generalities

Over the last decades, β-decay properties of light unstable nuclei have been extensively investigated in order to probe their single-particle nuclear structure and to establish the proton and neutron drip-lines. Hence, compilations of spectroscopic properties are available for many sd shell nuclei [1,2,3,4,5] from which nucleon-nucleon interactions were derived [6]. β-decay studies of nuclei having a large proton excess are therefore useful to test the validity of these models when they are applied to very unstable nuclei.

Moreover, in the standard $V-A$ description of β decay, a direct link between experimental results and fundamental constants of the weak interaction is given by the reduced transition probability ft of the individual allowed β decays. This parameter, which incorporates the phase space factor f and the partial half-life $t = T_{1/2}/BR$ ($T_{1/2}$ being the total half-life of the decaying nucleus and BR the branching ratio associated with the β transition considered), can be written as follows:

$$ft = \frac{\mathcal{K}}{g_V^2 |< f|\tau|i >|^2 + g_A^2 |< f|\sigma\tau|i >|^2} \qquad (1)$$

where $\mathcal{K}$ is a constant and where g_V and g_A are, respectively, the vector and axial-vector current coupling constants related to the Fermi and Gamow-Teller components of β decay. τ and σ are the isospin and the spin operators, respectively. Hence, the comparison of the measured ft values and the computed Fermi and Gamow-Teller matrix elements appears to be a good test of nuclear wave functions built in the shell-model frame, stressing the role of the overlap between initial and final nuclear states as well as the configuration mixing occurring in parent and daughter states. However, two systematic deviations from theoretical predictions show the limitation of our theoretical understanding and treatment of fundamental interactions. They are reported as the *mirror asymmetry anomaly in β decay* [7,8,9,10] and the *quenching of the Gamow-Teller strength* [11,12,13].

Mirror asymmetry in β decay: This phenomenon is related to the isospin non-conserving forces acting in the atomic nucleus. If nuclear forces were charge independent, the β^+ (EC) and the β^- decays of analog states belonging to mirror nuclei would be of equal strength. The deviation from this simple picture is characterized by the asymmetry parameter $\delta = (ft^+/ft^- - 1)$, where the $+$ and $-$ signs are associated with the decay of the proton- and the neutron-rich members of

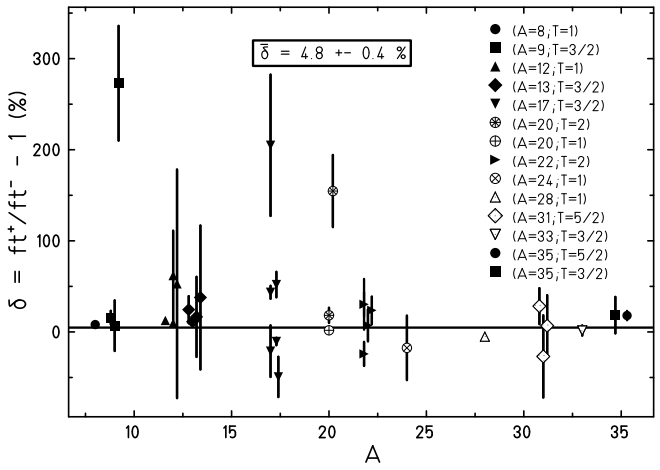

Fig. 1. Systematics of the experimental values of the asymmetry parameter δ for nuclei with $A \leq 40$. Only allowed Gamow-Teller transitions with $log(ft) \leq 6$ are considered.

the mirror pair, respectively. Figure 1 presents an updated systematics of δ values measured for mirror nuclei with $A \leq 40$. 39 allowed Gamow-Teller mirror transitions with $log(ft) \leq 6$ pertaining to 14 pairs of nuclei are analyzed (see ref. [14] for details). They lead to a mean deviation of about $5\,\%$ for these nuclei lying in the p and sd shells. The asymmetry reaches $11\,(1)\,\%$ if only p shell nuclei are considered, which stresses the interplay between the Coulomb and the centrifugal barriers.

It was often attempted to explain the mirror asymmetry anomaly in the p shell either in terms of binding energy effects [8,9,15] or by introducing the concept of "second class currents" [16,17,18], which are not allowed within the frame of the standard V-A model of the weak interaction. None of the theoretical approaches were able to reproduce the measured δ values. Shell-model calculations are currently performed to test the isospin non-conserving part of the interaction in β decay by studying the influence of isospin mixing effects and of radial overlap mismatches of nuclear wave functions on the Gamow-Teller matrix elements. These calculations are performed in the p shell and in the sd shell, where reliable single-particle nuclear wave functions are now available [7].

Gamow-Teller quenching: The axial-vector coupling constant g_A involved in β transitions of the Gamow-Teller type is not strictly constant and it has to be renormalized in order to reproduce the ft values measured experimentally [19]. The effective coupling constant $g_{A,eff} = q{*}g_A$ is deduced empirically from nuclear structure experiments and shows a slight variation over a wide range of masses: $q = 0.820\,(15)$ in the p shell [20], $q = 0.77\,(2)$ in the sd shell [21] (giving a quenching factor q^2 of 0.6) and $q = 0.744\,(15)$ in the pf shell [22].

Different theoretical approaches have been used in order to derive the renormalization factor from core polarization effects (due to particle-hole excitations), isobar currents and meson exchange [23]. Despite all these efforts, the origin of the quenching effect is not very well understood. Nevertheless, the Gamow-Teller strength function $B(GT) = (g_A/g_V)^2\,|\sigma\tau|^2$, which translates the global response of the wave function to spin-isospin excitations occurring in β decay, is a useful link between experimental results and theoretical predictions and it can be used as a comparative tool.

Experimental development: With the development of secondary radioactive beams and other experimental techniques like the combination of helium-jet transport systems with telescope detectors [24,25,26], a large set of neutron-deficient nuclei has been investigated since the β-delayed proton emission was first observed forty years ago [27]. As Q_{EC} values are increasing while nuclei become more exotic, $\beta - p$ and $\beta - \gamma$ spectroscopic studies of neutron-deficient nuclei give the opportunity to probe the Gamow-Teller strength function up to more than 10 MeV in excitation energy. Hence, the whole energy window open in β decay can be covered both by spectroscopic studies and charge exchange reactions [28]. Therefore, the theoretical description of nuclear structure as well as our understanding of the weak interaction can be tested far from the stability line. As an illustration, we will report in the following on the β-decay properties of two neutron-deficient light nuclei, namely ^{25}Si and ^{26}P.

1.2 Previous studies

1.2.1 Studies of ^{25}Si

With a lifetime of 218 ms and a Q_{EC} value of about 13 MeV, the $T_Z = -\frac{3}{2}$ nucleus ^{25}Si has been studied several times since the end of the 1960's. These previous studies will be used in the present work to validate the analysis procedure implemented to derive the β-decay properties of ^{26}P. However, none of these studies measured the decay by γ emission of excited states fed in the β decay of ^{25}Si.

The most recent β-delayed proton emission study of ^{25}Si was performed by Robertson *et al.* [26]. It updates the first investigation of Reeder *et al.* in 1966 [29]. In both experiments, the individual proton group intensities were measured relative to the most intense one, emitted by the isobaric analog state (IAS) in ^{25}Al. The absolute β-decay branching ratio of $12.2\,\%$ towards this state was derived from the associated $log(ft)$ value ($log(ft) = 3.28$), calculated assuming a pure Fermi β transition from the ground state of ^{25}Si. It led to a summed β feeding of proton-unbound states of ^{25}Al equal to $38.1\,(15)\,\%$. This normalization procedure is supported by the measurement of Hatori *et al.* [12]. In this work, absolute branching ratios for β decay were determined by counting the total number of β particles emitted with the half-life of ^{25}Si and the β feeding of the IAS in ^{25}Al was indeed found to be equal to $14.6\,(6)\,\%$, giving rise to a $log(ft)$ value of $3.19\,(2)$. The summed feeding of the ^{25}Al proton-emitting states was measured to be $40.7\,(14)\,\%$, in good agreement with Robertson *et al.*

As mentioned above, in none of the experiments, the β-delayed γ decay of ^{25}Si was observed. As a consequence, the β-decay branching ratios towards the proton-bound states of ^{25}Al were tentatively estimated taking into account the summed

β feeding and assuming that the relative ft values of these states were equal to those of the mirror states in ^{25}Mg. The weak point of such a procedure is that an average β asymmetry of $20\,\%$ had to be taken into account for all proton-bound state, which was assumed to be equally shared by the proton-bound states disregarding their individual quantum characteristics.

1.2.2 Studies of ^{26}P

Due to its T_Z value of -2 and its short lifetime of less than $100\,ms$, ^{26}P has not been investigated in detail so far. Compilations only report the observation by Cable *et al.* of β-delayed proton and two-proton emission from this nucleus [25,30]. A half-life of $20^{+35}_{-15}\,ms$ was deduced from the observation of the most intense proton group. It led to a β feeding of the IAS in ^{26}Si equal to $1.9^{+3.5}_{-1.4}\,\%$ using a calculated $log(ft)$ value of 3.19 (assuming a pure Fermi transition). Only three proton groups were observed linking the IAS to the two lowest states of ^{25}Al ($\beta-p$ decay) and to the ground state of ^{24}Mg ($\beta-2p$ decay). The two decay modes of the IAS were reported to be of similar magnitude. However, the large Q_{EC} value of $18\,MeV$ together with a proton separation energy of $5.5\,MeV$ for the daughter nucleus ^{26}Si are indications that the β-delayed charged-particle spectrum may be rather complex, involving a large number of proton groups.

1.3 Present measurements

In our experiment, we determined the absolute branching ratios for ^{25}Si and ^{26}P by relating the intensity of a given proton or γ line to the number of isotopes of each type implanted in our set-up. For ^{25}Si, this measurement constitute a first unambigous determination of branching ratios also for proton-bound levels. We will use the decay of ^{25}Si in part to test our analysis procedure, however, our study yields also new results for this nucleus, in particular for the γ decay of its β-decay daughter. In the case of ^{26}P, we deduce for the first time the feeding for other states than the IAS and their decay by proton or γ emission. Therefore, we could establish a complete decay scheme for branches with more than about 1% feeding for both nuclei for the first time.

2 Experimental procedure

2.1 Fragment production and detection set-up

In addition to ^{25}Si and ^{26}P, the β-delayed proton and two-proton emitters ^{22}Al [31] and ^{27}S [32] have been studied during the same experimental campaign. The β-delayed proton emitter ^{21}Mg [24] and the β-delayed γ emitter ^{24}Al [4] were also produced for calibration and efficiency measurement purposes.

All nuclei have been produced in the fragmentation of a 95 MeV/u ^{36}Ar^{18+} primary beam with an intensity of about $2\mu Ae$ delivered by the coupled cyclotrons of the GANIL facility. A $357.1\,mg/cm^2$ ^{12}C production target was placed in the SISSI device [33], the high angular acceptance and focusing properties of which increased the selectivity of the fragment separation operated by the LISE3 spectrometer. The latter included a shaped Be degrader (thickness 1062μm) at the intermediate focal plane and a Wien filter at the end of the line to refine the selection of the separated fragments.

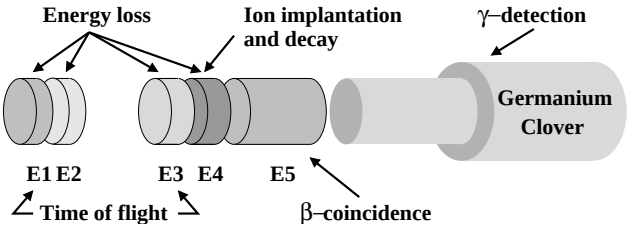

Fig. 2. Schematic view of the identification and detection set-up. It includes a germanium detector and five silicon detectors mounted in close geometry, where selected ions were identified by means of energy-loss and time-of-flight measurements. The last two detectors were used to observe the charged particles emitted in decay events in the implantation detector $E4$.

nucleus	production rate (pps)	contamination (%)	implanted ions ($*10^3$)
^{25}Si	300	< 1	492 (1)
^{26}P	65	≈ 13	2180 (70)

Table 1. Production rate, contamination and total number of selected ions during the experiment.

Ions of interest were implanted in the fourth element $E4$ of a silicon stack (figure 2). The ion identification was performed by means of time-of-flight and energy-loss measurements with the silicon detectors $E1$ to $E4$ ($2*300\,\mu m$ and $2*500\,\mu m$ in thickness, $4*600\,mm^2$ of surface). It led to a precision in the counting rate of better than $1\,\%$ for ^{25}Si and about $3\,\%$ for the more exotic ^{26}P nucleus. The production method in association with the high selectivity of the LISE3 spectrometer gave rise to a very low contamination rate of the selected species by only a few isotones (see table 1).

Protons were detected in the implantation detector $E4$, in coincidence with the observation of β particles in the detector $E5$ (with a thickness of $6\,mm$ and an area of $600\,mm^2$). A segmented germanium clover was finally used to study the β-delayed γ decay of implanted ions.

2.2 β-delayed proton spectroscopy

Contrary to previous experiments [24,25,26] in which ions were deposited at the surface of an ion catcher, β-delayed protons are emitted inside the implantation detector $E4$. As a first consequence, the proton spectrum rises on a large β background and the identification of low-energy, low-intensity proton lines is difficult. Secondly, the energy deposit in the detector $E4$ of an emitted proton cannot be disentangled from the energy-loss contribution of the associated β particle and the recoiling ion.

To minimize these effects, ions were implanted in the last $100\,\mu m$ of the detector $E4$ and a β coincidence with the thicker

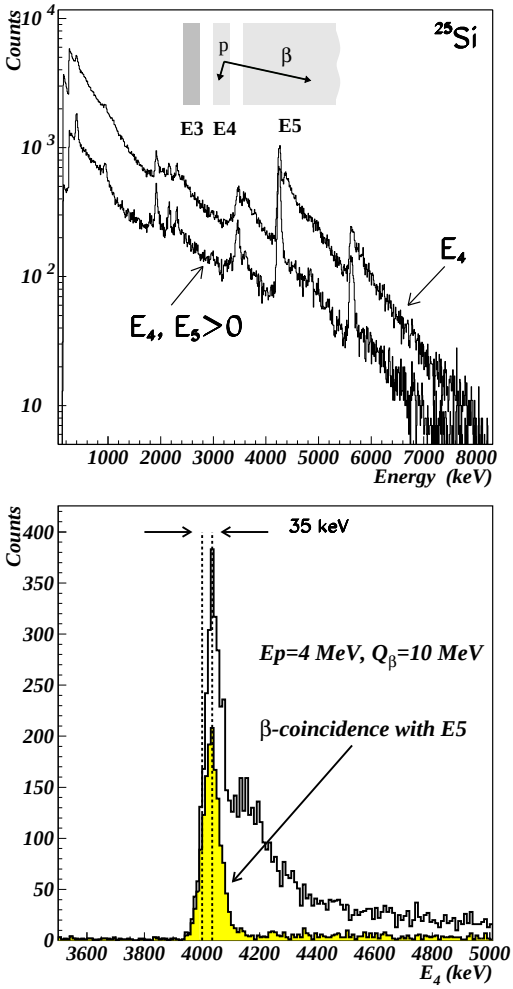

Fig. 3. The upper part of the figure shows the influence of the β-coincidence condition ($E5 > 0$) on the energy spectrum delivered by the detector E4 for the setting on ^{25}Si. The lower part of the figure presents a GEANT simulation of the effect of the coincidence condition on the shape of a β-delayed proton emission peak. The dotted lines show the $35keV$ energy shift due to the β pile-up, i.e. a $4MeV$ proton peak is in fact observed at an energy of $4.035MeV$. This shift depends on the implantation depth and varies for the different nuclei studied in this work. The coincidence condition does not alter this shift significantly.

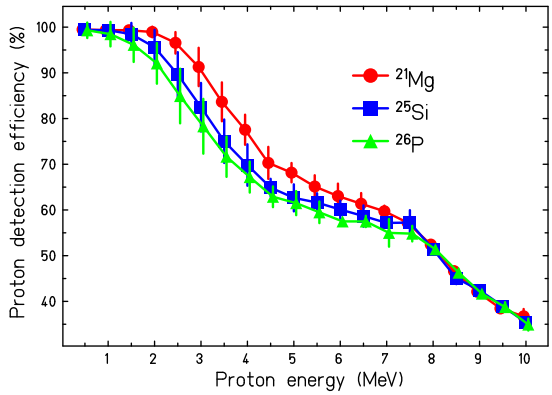

Fig. 4. GEANT simulation of the proton detection efficiency of the implantation detector $E4$. The error bars on the plotted data are deduced from different parametrizations of the ion implantation profiles. An uncertainty due to the detector thickness is not included, as it is of the same order of magnitude as the uncertainty of the implantation profile. (see text for details).

detector $E5$ was requested in the analysis. As shown in the upper part of figure 3, the β particle energy deposit in the coincidence spectrum was strongly reduced and proton peaks could be easily identified and fitted with the help of Gaussian distributions. The energy calibration of the detector $E4$ as well as the measurement of the proton group intensities were performed on the basis of this $E4$-$E5$ coincidence condition.

2.2.1 Energy calibration of the implantation detector

The β particle energy deposit leads to a shift in energy of the Gaussian-like part of the proton peaks. This effect could be reproduced by means of a GEANT simulation [34], as shown in the lower part of figure 3 for a representative β-delayed proton peak. It could also be shown that the energy shift is roughly independent on the proton and β-particle energies but linearly dependent on the implantation depth of the ions, that is to say, on the distance the β particles travel in the detector $E4$ before leaving it to enter the coincidence detector $E5$. The energy calibrations of the detector $E4$ for the settings on ^{21}Mg, ^{25}Si and ^{26}P were therefore assumed to differ only by a shift proportional to the implantation depths of the ions.

The calibration parameters for the settings were deduced from the identification of the major proton groups expected at $1315\,(9)$, $1863\,(2)$, $2037\,(4)$, $2589\,(9)$, $4908\,(3)$ and $6542\,(3)$ keV for the decay of ^{21}Mg [24] and at $402\,(1)$, $1925\,(3)$, $2169\,(7)$, $2312\,(4)$, $3472\,(10)$, $4261\,(2)$ and $5630\,(2)$ keV for the decay of ^{25}Si [26]. The proton group energies were recalculated using the excitation energies of the proton-emitting states and the proton separation energies reported in a compilation [4].

2.2.2 Proton detection efficiency

Since ions were implanted at the end of the detector $E4$, the proton detection efficiency $\mathcal{E}_p$ is very sensitive to the implantation profile of the emitting ion and to the proton energy. The detection efficiency for protons between 0.5 and $10\,MeV$ was computed by means of GEANT simulations. Following experimental observations, implantation profiles were approximated by Gaussian distributions in the beam direction (with a standard deviation of $20\,\mu m$) and with a two dimensional square shaped function in the orthogonal plane [35].

Results are shown in figure 4. An uncertainty on the detection efficiency of less than 6 % was obtained. This uncertainty was determined by varying the implantation depth by $\pm\,10\,\mu m$, which is roughly the width of the implantation distribution.

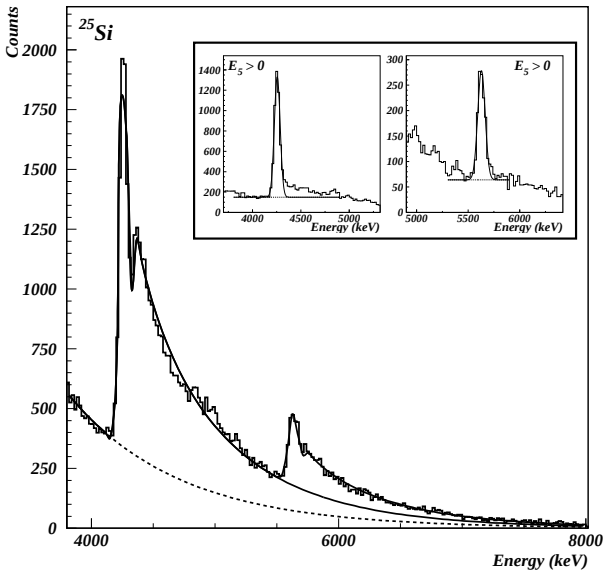

Fig. 5. High energy part of the β-delayed proton spectrum in the decay of ^{25}Si. The areas of the two main proton peaks above $4\,MeV$ obtained with (inset) and without (main figure) coincidence condition were used to extract an average normalization factor Kc_p for the setting on ^{25}Si.

2.2.3 Absolute intensities of the observed proton groups

The absolute intensity I_p^i of a given proton group i was derived from the following relation:

$$I_p^i = \frac{Sc_p^i}{Kc_p * N_{impl} * \mathcal{E}_p^i} \qquad (2)$$

where Sc_p^i is the area of the proton peak observed in the coincidence spectrum ($E_5 > 0$), Kc_p the normalization factor to be taken into account due to the coincidence condition, N_{impl} the number of ions implanted in $E4$ and $\mathcal{E}_p^i$ the proton detection efficiency for a given proton energy.

The extraction of the factor Kc_p is illustrated in figure 5 for the setting on ^{25}Si. Several proton peaks were fitted in the high energy part of the $E4$ energy spectrum, where the β background is low enough and where proton peaks are well separated. The Kc_p coefficients were deduced from the average ratio of the areas of the β-delayed proton peaks obtained with and without coincidence condition. For the coincidence spectrum, peaks were fitted by means of Gaussian distributions on a linear background (see inserts of figure 5) leading to the Sc_p^i values. For the unconditioned energy spectrum, fit functions convoluting a Gaussian distribution and an exponential tail on top of an exponential background were used. For each ion of interest, the parameters of the exponential tail were fixed regardless of the proton peak energies. The Kc_p coefficients obtained were about $13\,\%$, with an uncertainty of 1 to 2%.

2.3 γ-ray spectroscopy

As shown in figure 2, a segmented germanium clover detector was placed at 0 degree, a few centimeters away from the silicon stack. To reduce the dead time of the acquisition system, the γ-ray signals were not used to trigger the data acquisition. As a consequence, the probability to observe a γ decay depended on the type of radioactivity event that had triggered the acquisition system. Since the energy loss of a proton in $E4$ was larger than a few hundred keV, a trigger signal was obtained each time a proton was emitted. Subsequent γ rays were then automatically detected, depending only on the Germanium detector efficiency.

On the other hand, most of the β particles emitted without accompanying protons did not lose enough energy in $E4$ to trigger the acquisition system. As a consequence, the trigger efficiency for β-γ events was given mainly by the fraction of the total solid angle under which the large silicon detector $E5$ is seen from $E4$. This efficiency was determined by means of ^{24}Al which decays by β-γ emission. The absolute intensities of the two main γ lines at 1077 and $1369\,keV$ were measured and compared with the expected values [4]. The β-trigger rate was then derived, taking into account the intrinsic efficiency of the Germanium detector, which was obtained with conventional calibration sources. The overall γ-detection efficiency in the 300 to $2000\,keV$ range was about 2 to $3\,\%$, with a relative uncertainty of about $20\,\%$. The β-trigger efficiency was equal to $35.0\,(45)\,\%$.

To a large extent, corrections due to true summing effects [36] were included in the calculated β-trigger rate. However, this effect was not under control when the acquisition was triggered by the detection of protons, where the trigger efficiency was 100%. Hence, γ-ray intensities could not be determined reliably for $\beta - p - \gamma$ decay events and therefore β-decay branching ratios towards proton-emitting states could not be cross-checked by means of γ spectroscopy.

3 Experimental results

The β-decay properties of ^{25}Si are compared in the following to the results obtained in previous work. For the two settings on ^{25}Si and on ^{26}P, the relative intensities of the identified proton groups are given as well as the deduced absolute β-decay branching ratios towards the proton-unbound nuclear states of the daughter nuclei. The analysis of β-delayed γ spectra gives rise, for the first time, to the measurement of the absolute feeding of the proton-bound states. The decay schemes are then proposed and compared to calculations performed in the full sd shell by Brown [37] with the OXBASH code [38] using the USD interaction [6]. Finally, the Gamow-Teller strength distributions are compared to those expected from the mirror β decays and to those extracted from the calculated $log(ft)$ values. The main characteristics of ^{26}P are given, including a precise measurement of its lifetime as well as a derivation of its proton separation energy S_p and of its atomic mass excess $\Delta\,(^{26}P)$.

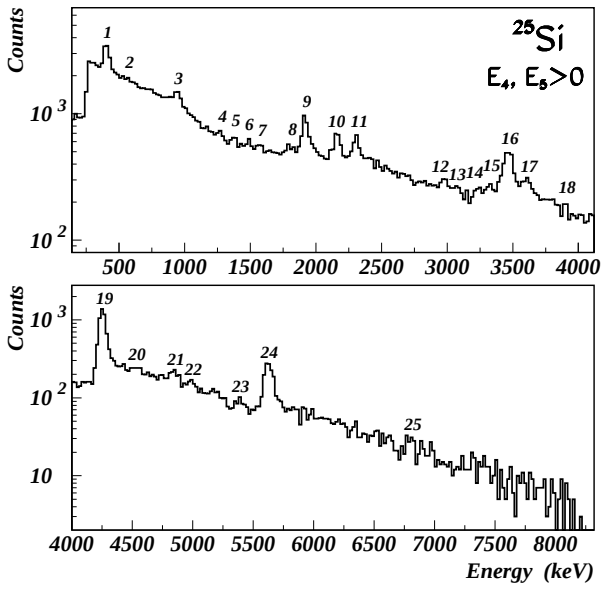

Fig. 6. β-delayed proton spectrum obtained in coincidence with a signal in $E5$ in the decay of ^{25}Si. The peak labels correspond to the peak numbers used in tables 2 and 3.

3.1 β-decay study of ^{25}Si

3.1.1 β-delayed proton emission

The β-delayed proton emission spectrum obtained in coincidence with the detector $E5$ is shown in figure 6 for the setting on ^{25}Si. Most of the proton groups reported in previous work by Robertson *et al.* [26] and Hatori *et al.* [12] have been identified. Their center of mass energies and their relative intensities are compared in table 2 and discussed in the following.

Missing transitions: Nine of the thirty-two proton groups reported by Robertson *et al.* were not observed in the present work. Six of these transitions (see table 2) were already not observed in the work of Hatori *et al.* and it is therefore plausible that they are due to the decay of β-p contaminants in the experiment performed by Robertson *et al.*. The three remaining missing transitions have a relative intensity lower than $1\,\%$ and it may be that the residual β background in the spectrum conditioned by $E5$ is too large in the present experiment to allow for their identification.

Identification of the observed proton groups: All the observed proton groups were attributed to proton transitions reported in the work of Robertson *et al.* on the basis of their measured center of mass energies. Two groups at $2980\,(9)$ and $3899\,(2)\,keV$ were tentatively identified as being the same transitions as those at $3021\,(9)$ and $3864\,(20)\,keV$ by Robertson *et al.* although the energy differences are about $40\,keV$. The proton group at $401\,(1)$ in the present work corresponds most likely to the $382\,(20)\,keV$ group of Robertson *et al.* because of their high relative intensities. The transition at $1377\,(6)\,keV$ was attributed to an emission from the IAS of ^{25}Al and was therefore identified as the transition at $1396\,(20)\,keV$ of Robertson *et al.* The same is most likely true for the transitions at $1573\,(7)$ and $1592\,(20)\,keV$. The proton group at $3326\,(6)\,keV$ was observed at the same energy as in the work of Hatori *et al.* and corresponds most likely to the transition at $3342\,(15)\,keV$ in reference [26]. All other transitions identified were measured at energies differing by less than $15\,keV$ with respect to the work of Robertson *et al.*

High-energy proton groups: Only one of the three high energy transitions reported by Zhou *et al.* [39] was identified at $6802\,(7)\,keV$. Its relative intensity of $2.2\,(5)\,\%$ is significantly higher that the values given in references [12] and [39], which might reflect an underestimation of the proton detection efficiency at high energies in the present work.

New transition: A new proton transition at $3077\,(14)\,keV$ (label 13) was observed but could not be attributed. Due to its low intensity of $0.25\,(11)\,\%$, the transition could not be assigned neither by means of a $\beta-p-\gamma$ coincidence nor by any other means.

Assignment of proton transitions: Apart from the transition at $3326\,keV$ which, according to Hatori *et al.*, originates from the $5597\,keV$ excited level in ^{25}Al, all identified proton groups were assigned following the work of Robertson *et al.* The deduced energies and absolute β-decay branching ratios of the proton-unbound states of ^{25}Al are presented in table 3. The obtained excitation energies are compared to the data of the compilation [5]. Large discrepancies of more than $25\,keV$ are found for the proton groups at 2980, 3899 and $5407\,keV$. The IAS of ^{25}Al was found at an excitation energy of $7892\,(2)\,keV$, in agreement with the value of $7896\,(6)$ reported by Robertson *et al.* [26].

The overall agreement between the three β-delayed proton decay studies of ^{25}Si is reasonable, leading to a summed β-decay branching ratio towards the proton unbound states of ^{25}Al equal to $35\,(2)\,\%$ (this work), $38\,(2)\,\%$ [26] and $41\,(1)\,\%$ [12]. The difference originates for a large part from the determination of the absolute intensity of the least energetic proton group at about $400\,keV$ in the center of mass. This proton transition is reported in the previous work to compete with a γ deexcitation of the associated nuclear state, but no evidence was found in the γ-decay spectrum for such a decay mode.

Regarding the absolute β feeding of the IAS in ^{25}Al, the value of $12.8\,(8)\,\%$ obtained in this work is in good agreement with the theoretically expected value of $12.2\,\%$ used by Robertson *et al.* and is significantly lower than the one measured by Hatori *et al.* It leads to a $log(ft)$ value of $3.25\,(3)$ for the β decay of ^{25}Si towards the IAS in ^{25}Al. This result confirms the assumption that the involved β transition is almost purely of the Fermi type, since a $log(ft)$ value of 3.28 is expected in this case [26].

3.1.2 β-delayed γ decay

The γ-ray spectrum obtained in the decay of ^{25}Si is shown in figure 7. The four γ lines at 452 (absolute branching ratio of $18.4\,(42)\,\%$), 493 ($15.3\,(34)\,\%$), 945 ($10.4\,(23)\,\%$) and $1612\,keV$ ($15.2\,(32)\,\%$) were assigned to the β-delayed γ decay of ^{25}Si. The last γ line is a doublet of two γ rays from the decay of the $\frac{7}{2}^+_1$ states at $1612.4\,keV$ in ^{25}Al and at $1611.7\,keV$ in its daughter nucleus ^{25}Mg [4]. Taking into account the ex-

This experiment				Robertson *et al.* [26]			Hatori *et al.* [12]	
Peak	C.M. Energy (keV)	Relative intensity (%)	Absolute intensity (%)	Peak	C.M. Energy (keV)	Relative intensity (%)	C.M. Energy (keV)	Relative intensity (%)
1	401 (1)	49.8 (48)	4.75 (32)	1	382 (20)	73.7 (3)	403 (1)	57.7 (63)
2	555 (11)	7.2 (27)	0.69 (25)	2	550 (25)	< 2.5 (1)		
3	943 (2)	17.1 (24)	1.63 (20)	3	943.4 (−)	17 (1)	945 (2)	11.5 (24)
				4	1040 (20)	1.53 (3)		
4	1268 (6)	6.1 (18)	0.58 (17)	5	1272 (20)	2.26 (7)		
5	1377 (6)	4.3 (12)	0.41 (11)	6	1396 (20)	2.89 (5)		
6	1489 (7)	5.0 (15)	0.48 (14)	7	1501 (20)	2.90 (5)		
7	1573 (7)	4.3 (13)	0.41 (12)	8	1592 (20)	1.46 (3)	1586 (3)	2.1 (9)
				9	1685 (20)	0.93 (6)		
8	1804 (8)	6.1 (14)	0.58 (13)	10	1805 (15)	6.73 (6)	1791 (3)	5.4 (10)
9	1917 (2)	23.5 (27)	2.24 (21)	11	1925.2 (−)	27.4 (1)	1925 (3)	17.6 (13)
10	2162 (4)	18.1 (26)	1.73 (22)	12	2165 (10)	17.2 (1)	2169 (7)	12.8 (11)
11	2307 (4)	16.5 (25)	1.57 (21)	13	2311.4 (−)	14.1 (1)	2312 (4)	11.2 (9)
				14	2373 (20)	2.02 (3)		
				15	2453 (25)	0.40 (2)		
				16	2486 (25)	0.96 (2)	2483 (?)	< 1.4
				17	2608 (25)	0.39 (5)	2636 (10)	0.5 (2)
12	2980 (9)	1.7 (7)	0.16 (7)	18	3021 (15)	3.74 (9)	3022 (9)	5.0 (14)
13	3077 (14)	2.6 (12)	0.25 (11)					
14	3231 (8)	5.4 (13)	0.51 (12)	19	3237 (15)	4.15 (5)	3243 (10)	2.4 (6)
15	3326 (6)	5.9 (12)	0.56 (11)	20	3342 (15)	6.57 (6)	3356 (30)	44.7 (48)
16	3463 (3)	28.1 (34)	2.68 (26)	21	3466 (10)	34.5 (1)	3472 (10)	
17	3610 (11)	5.9 (18)	0.56 (17)	22	3597 (10)	10.86 (8)	3608 (5)	13.3 (18)
18	3899 (2)	3.4 (7)	0.32 (6)	23	3864 (20)	1.15 (7)	3852 (8)	3.9 (12)
19	4252 (2)	100 (10)	9.54 (66)	24	4258.3 (−)	100 (2)	4261 (2)	100
				25	4303 (20)	3.32 (7)		
20	4545 (10)	6.6 (18)	0.63 (17)	26	4556 (20)	1.28 (5)	4552 (8)	1.3 (6)
				27	4626 (25)	0.25 (1)	4612 (10)	0.4 (4)
21	4850 (6)	10.3 (17)	0.98 (15)	28	4853 (15)	7.29 (7)	4841 (5)	16.7 (18)
22	4986 (8)	< 4.9 (9)	< 0.47 (8)	29	4992 (15)	2.30 (4)	4977 (5)	1.4 (4)
23	5407 (7)	3.6 (7)	0.34 (6)	30	5394 (20)	1.98 (5)	5366 (6)	0.8 (3)
				31	5549 (15)	3.19 (6)		
24	5624 (3)	25.1 (27)	2.39 (20)	32	5630 (10)	16.9 (2)	5630 (2)	21.1 (15)
25	6802 (7)	2.2 (5)	0.21 (4)	ref. [39]	6520 (10)	0.72 (4)	6795 (17)	0.7 (3)

Table 2. β-delayed proton emission of ^{25}Si. The center of mass energy and the relative intensity of the identified proton groups are compared to previous experimental data. The relative and absolute intensities of the β-delayed proton transitions obtained in this work are also reported.

pected contribution of this second transition in ^{25}Mg, the absolute intensity of the $1612\,keV$ γ ray in ^{25}Al was deduced to be equal to $14.7\,(32)\,\%$.

The γ lines at 493 and $945\,keV$ are associated with the de-excitation of the $\frac{3}{2}^+_1$ state at $945\,keV$ in ^{25}Al towards its $\frac{5}{2}^+_1$ ground state and towards the $\frac{1}{2}^+_1$ excited state at $452\ keV$. The intensity ratio of the two lines $I_\gamma(945)/I_\gamma(493) = 68\,(26)\,\%$ is in agreement with the value of $79\,(6)\,\%$ obtained in an in-beam experiment [4].

Since the intensities of the 493 and $452\ keV$ γ rays were found to be equal within their uncertainties, we conclude that the $452\ keV$ state is not fed directly in the β decay of ^{25}Si. Such a β transition would be indeed a first-forbidden one and is therefore unlikely to be observed in the present experiment.

No γ rays were observed at 845, 1338 and $1790\,keV$. Therefore, it was assumed that the $\frac{7}{2}^+_2$ proton-bound state of ^{25}Al at $1790\,keV$ [5] is not fed in the β decay of ^{25}Si. Hence, the measurements of the absolute intensities of the three γ lines at 493, 945 and $1612\,keV$ led to a summed β-decay branching ratio towards the proton-bound excited states of ^{25}Al of $41\,(5)\,\%$ (see table 4 for details). Taking into account the previously determined summed β-decay branching ratio towards the proton-unbound states ($35\,(2)\,\%$), this leads to an absolute β feeding of the ^{25}Al ground state of $24\,(7)\,\%$.

The γ line observed at $1369\,keV$ corresponds to the de-excitation of the first excited state of ^{24}Mg populated in the $\beta{-}p$ decay of ^{25}Si. Due to the quite low γ-detection efficiency and the weakness of most of the proton transitions feeding excited states of ^{24}Mg, neither the $4^+_1 \rightarrow 2^+_1$ nor the $2^+_2 \rightarrow 4^+_1$ transitions were seen. Only a few counts at an $E4$ energy of about $4.25\,MeV$ were observed in coincidence with the γ ray at $1369\,keV$, in agreement with the assignment of the strongest proton group to the IAS in ^{25}Al. The γ line at $1461\,keV$ is the well-known background γ ray from ^{40}K.

C.M. proton energies (keV) in the decay to ^{24}Mg states				Excitation energies and β feeding (B.R.) of ^{25}Al proton-unbound states		
Ground state	1369 keV	4123 keV	4238 keV	This work	ref. [5]	B.R. (%)
1−401 (1)				2672 (1)	2673.5 (6)	4.8 (3)
7−1573 (7)				3844 (7)	3858.8 (8)	0.4 (1)
9−1917 (2)	2−555 (11)			4189 (2)	4196 (3)	2.9 (3)
11−2307 (4)	3−943 (2)			4582 (2)	4583 (4)	3.2 (3)
	4−1268 (6)			4908 (6)	4906 (4)	0.6 (2)
15−3326 (6)				5597 (6)	5597 (5)	0.56 (11)
	10−2162 (4)			5802 (4)	5808 (6)	1.7 (2)
18−3899 (2)				6170 (2)	6122 (3)	0.32 (6)
	12−2980 (9)			6620 (9)	6645 (4)	0.16 (7)
	14−3231 (8)			6871 (8)	6881 (6)	0.5 (1)
21−4850 (6)	16−3463 (3)			7107 (3)	7121 (6)	3.7 (2)
22−4986 (8)	17−3610 (11)			7255 (7)	7240 (3)	$<$ 1.0 (6)
23−5407 (7)				7678 (7)	7637 (6)	0.34 (6)
24−5624 (3)	19−4252 (2)	6−1489 (7)	5−1377 (6)	7892 (2)	7902 (2)	12.8 (8)
	20−4545 (10)	8−1804 (8)		8193 (6)	8186 (3)	1.2 (2)
25−6802 (7)				9073 (7)	9065 (10)	0.21 (4)

Table 3. Excitation energies and β feeding of ^{25}Al proton-unbound nuclear states. Absolute branching ratios for the present work, which are deduced from the absolute intensity measurements of the β-delayed proton transitions, are given in the last column.

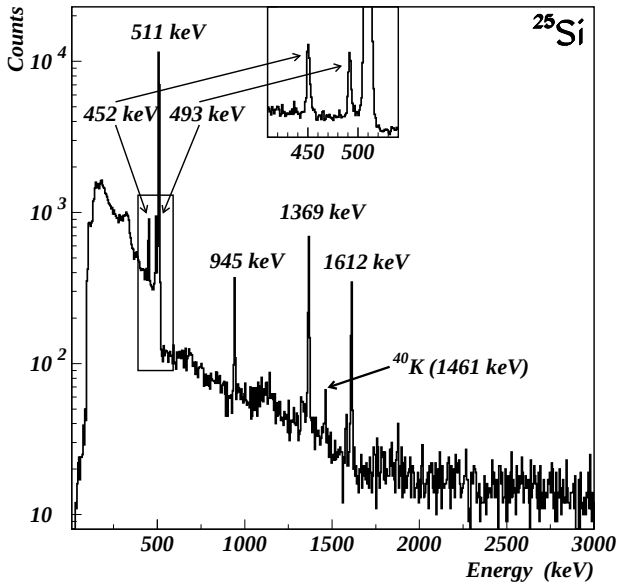

Fig. 7. ^{25}Si γ-decay spectrum. All γ lines except the one at 1461 keV are attributed to the decay of ^{25}Si.

3.1.3 β-decay scheme of ^{25}Si

Figure 8 shows the β-decay scheme proposed for ^{25}Si. The experimental branching ratios and the corresponding $log(ft)$ values are compared to shell-model calculations performed by Brown [37]. Only excited states predicted to be fed with a branching ratio of more than 0.1 % are taken into account. In terms of nuclear structure, the agreement between experimental results and theoretical calculations appears to be very good, most of the observed nuclear states being reproduced by the model within a few hundred keV.

states populated in ^{25}Al	Excitation energy (keV)	B.R. (%)
$\frac{5}{2}^+_1$	0	25 (7)
$\frac{3}{2}^+_1$	944.8 (4)	26 (4)
$\frac{7}{2}^+_1$	1612.4 (4)	15 (3)

Table 4. β-decay branching ratios towards proton-bound nuclear states of ^{25}Al.

The summed Gamow-Teller strength distribution as a function of the excitation energy of ^{25}Al is shown in figure 9. The experimental distribution is in good agreement with the one deduced from the shell-model calculations up to 6 MeV. Beyond, the model predicts the feeding of a lot of high-energy excited states by low intensity β transitions that are not visible experimentally. Due to the small phase-space factor f associated with such transitions, the related $B(GT)$ values are of importance, which explains the divergence at more than 6 MeV of excitation energy. The global agreement below 6 MeV is obtained for 11 individual β transitions for which the Gamow-Teller strength is quenched equivalent to a quenching factor of about 0.6.

At low excitation energy, the Gamow-Teller strength seems to be close to the one expected from the β decay of the ^{25}Si mirror nucleus, assuming that nuclear forces are isospin in-

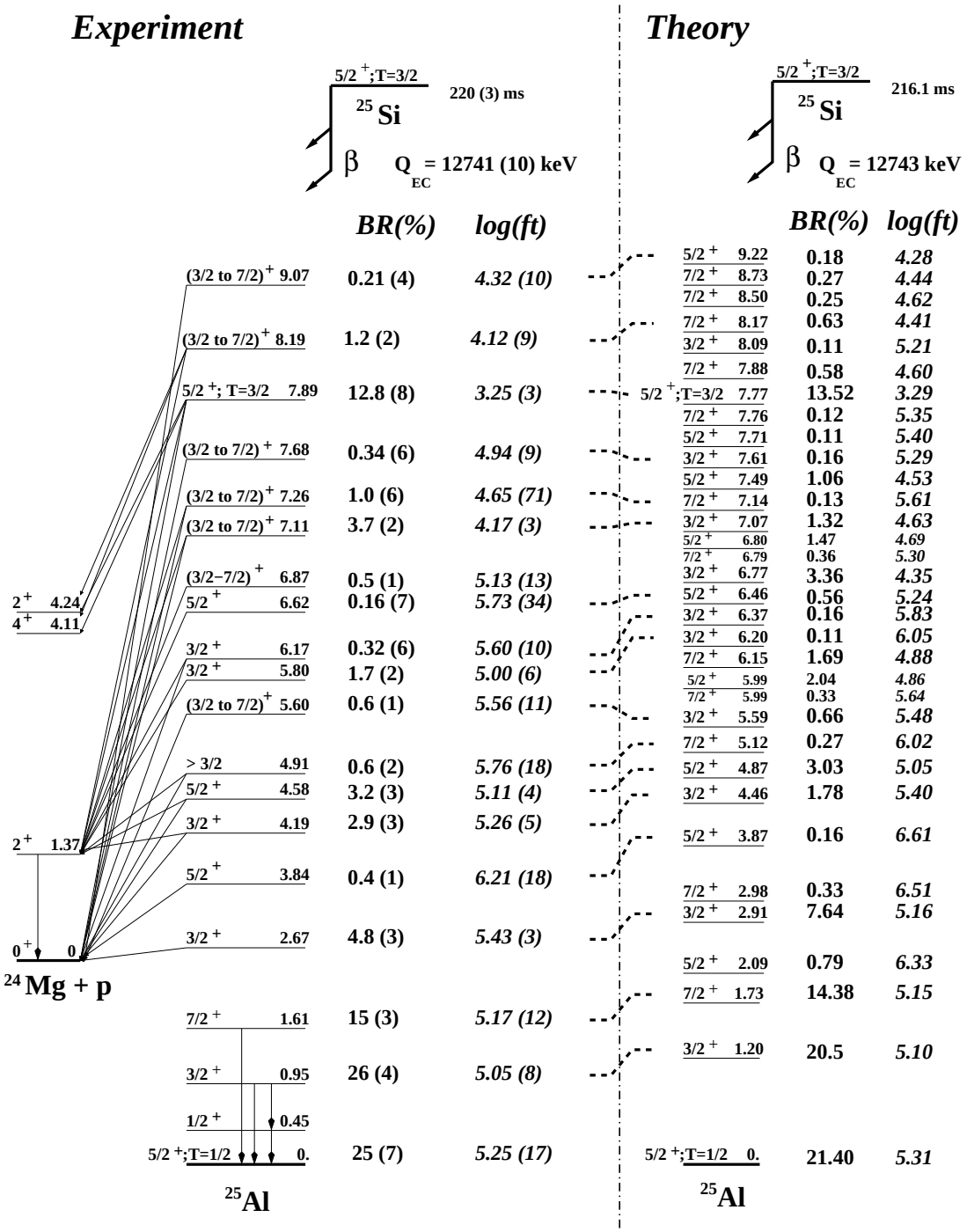

Fig. 8. β-decay scheme of ^{25}Si. Experimental results are compared to shell-model calculations performed by Brown [37] in the full sd shell with the USD interaction and the OXBASH code. The dotted lines tentatively connect experimentally determined levels to levels predicted by theory.

dependent ($\delta = 0$). Unfortunately, the error for the β-decay branching ratios towards these states is too large (see table 8 below) due to the uncertainty on the γ-detection efficiency and the individual values of the asymmetry parameter δ could not be derived precisely for the $(A=25, T=3/2)$ isospin multiplet (^{25}Na,^{25}Mg, ^{25}Al,^{25}Si).

3.2 β-decay study of ^{26}P

The experimental procedure established and tested with ^{25}Si is now applied to ^{26}P. The β-delayed proton spectrum conditioned by the detection of β particles in $E5$ is shown in figure 10. The contamination from other β-delayed proton emitters was determined from energy-loss and time-of-flight measure-

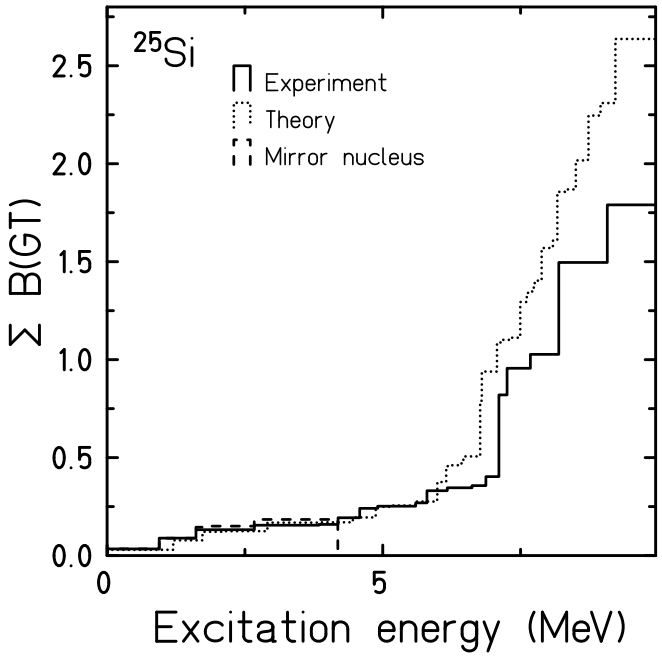

Fig. 9. Theoretical and experimental distributions of the summed Gamow-Teller strength ($\Sigma B(GT)$) for the decay of ^{25}Si. At low excitation energy, the distributions are also compared to the one obtained from the mirror β decay of ^{25}Na assuming isospin symmetry. The error of the Gamow-Teller strength distribution as determined in the present work is about 20%.

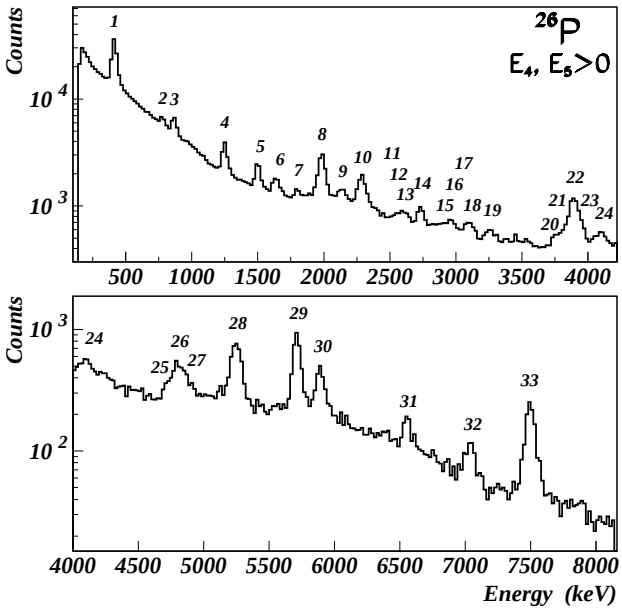

Fig. 10. β-delayed one-proton and two-proton spectrum obtained in coincidence with a signal in $E5$ in the decay of ^{26}P. The peak labels correspond to the peak numbers used in table 5.

ments to be $0.6\,\%$ for ^{27}S and $1.2\,\%$ for ^{25}Si. The most intense proton transition occurring in the decay of the latter nucleus is expected at $4.25\,MeV$. It was not observed in the present setting and all identified proton groups were therefore attributed to the decay of ^{26}P.

3.2.1 β-delayed proton emission

The center of mass energies as well as the relative and absolute intensities of the identified β-delayed proton or two-proton transitions are given in table 5. The large amount of produced nuclei allowed to performed $\beta-p-\gamma$ coincidences. Table 5 indicates the energy of the γ rays that were seen in coincidence with the corresponding proton peaks. All γ lines except the one at $1369\,keV$ are assigned to the decay of excited states of ^{25}Al. The γ ray at $1369\,keV$ is due to the β-delayed two-proton decay (transition 22, see below) of ^{26}P towards the first excited state of ^{24}Mg.

Proton and two proton emission of the IAS in ^{26}Si: By means of energy considerations and $\beta-p-\gamma$ coincidences, the five transitions labelled 29 to 33 could be assigned to the proton decay of the isobaric analog state in ^{26}Si. Its excitation energy was determined to be equal to $13015\,(4)\,keV$. Based on this first set of assignments, the two groups 22 and 28 were identified as two-proton transitions from the IAS to the first excited state and to the ground state of ^{24}Mg. The IAS excitation energy deduced from these two transitions is slightly higher in energy ($13036\,keV$ instead of $13015\,keV$) due to the lower pulse-height defect in two-proton emission. In the case of nearly back-to-back emission of the two protons, the recoil has an energy close to zero, whereas for parallel emission of the two protons, the recoil has a maxiumun energy comparable to one-proton emission. As the process of two-proton emission is supposed to be isotropic, the average recoil energy is about half compared to the one-proton emission value leading to a lower pulse height defect.

As described later, the determination of the excitation energy of the IAS was used to calculate the atomic mass excess of ^{26}P. The precise measurement of the ^{26}P lifetime (see below), and the summed β-decay branching ratio of $5.28\,(35)\,\%$ towards the IAS in ^{26}Si led to a $log(ft)$ value for this state of $3.13\,(5)$. This result is close to the expected model-independent value of 3.186.

Emission from known excited states of ^{26}Si: Due to their energy, transitions 3, 8, 12 and 13 were attributed to the decay of the previously observed excited states of ^{26}Si at $6350\,(25)$, $7489\,(15)$, $8570\,(30)$ and $8120\,(20)\,keV$ [4]. Although transition 12 is therefore expected to populate the first excited state of ^{25}Al, no γ ray at $452\,keV$ was observed in coincidence and the assignment of the transition is somewhat questionable. However, the intensity of this proton peak is rather weak which prevents most likely the observation of a coincident γ ray.

$\beta-p-\gamma$ coincidences: γ rays occurring in the deexcitation of ^{25}Al states were observed in coincidence with the proton groups labelled 5–7, 9–10, 16–21, 25 and 27. Therefore, these transitions were assigned to transitions between initial and final states based on $p-\gamma$ coincidences. No γ rays were seen in coincidence with the transitions 1, 2 and 4, although they are

Peak	C.M. Energy (keV)	Relative intensity (%)	Absolute intensity (%)	γ rays observed in coincidence
1	412 (2)	100.0 (71)	17.96 (90)	
2	778 (3)	4.3 (5)	0.78 (7)	
3	866 (2)	9.5 (10)	1.71 (15)	
4	1248 (2)	8.4 (8)	1.51 (12)	
5	1499 (2)	5.5 (5)	0.99 (7)	493, 945
6	1638 (3)	3.6 (4)	0.65 (6)	452
7	1798 (4)	1.1 (3)	0.20 (5)	452, 493
8	1983 (2)	13.3 (11)	2.39 (16)	
9	2139 (4)	3.0 (8)	0.54 (14)	452, 493, 1338
10	2288 (3)	8.2 (9)	1.47 (12)	1612
11	2541 (6)	0.5 (2)	0.09 (3)	
12	2593 (13)	1.5 (3)	0.27 (6)	
13	2638 (18)	0.6 (2)	0.11 (4)	
14	2732 (4)	2.6 (4)	0.47 (6)	
15	2855 (17)	$<$ 0.8 (2)	$<$ 0.14 (4)	
16	2908 (11)	0.3 (3)	0.06 (5)	452, 493
17	2968 (5)	1.8 (3)	0.32 (5)	452, 493
18	3097 (6)	1.7 (4)	0.31 (6)	452, 493, 845, 1790
19	3258 (4)	1.9 (2)	0.23 (4)	452, 493
20	3766 (9)	2.0 (4)	0.36 (7)	452
21	3817 (6)	0.7 (3)	0.13 (5)	452, 945
22	3879 (3)	4.4 (6)	0.79 (12)	1369
23	3920 (5)	6.7 (9)	1.21 (14)	
24	4097 (5)	$<$ 2.1 (3)	$<$ 0.37 (4)	
25	4719 (6)	1.3 (2)	0.24 (4)	452
26	4793 (3)	3.0 (4)	0.54 (6)	
27	4858 (4)	2.5 (3)	0.44 (5)	452
28	5247 (3)	7.6 (13)	1.37 (22)	
29	5710 (3)	7.8 (7)	1.40 (11)	452, 845, 1790
30	5893 (4)	4.1 (8)	0.73 (13)	1612
31	6551 (4)	1.2 (5)	0.21 (8)	452, 945
32	7039 (5)	1.0 (1)	0.17 (2)	
33	7494 (4)	3.4 (3)	0.61 (5)	

Table 5. β-delayed one-proton and two-proton emission of ^{26}P. The center of mass energy, the relative intensity and the absolute intensity of proton groups identified in figure 10 are given. The last column reports the γ rays observed in coincidence with the proton peaks. Transitions 22 and 28 are due to two-proton emission from the IAS of ^{26}Si.

quite intense. Hence, they were assumed to populate directly the ground state of ^{25}Al.

Assignments based on energy criteria: The excitation energies of the proton-emitting states in ^{26}Si derived from $\beta{-}p{-}\gamma$ coincidences were used to identify the proton groups 14, 23 and 26 as transitions from these states towards the ground state of ^{25}Al (c.f. table 6).

Unassigned proton transitions: The three transitions 11, 15 and 24 could not be assigned to the decay of excited states of ^{26}Si. Neither a coincident γ ray could be observed for these proton lines, nor their energy corresponds to an energy difference of identified levels. The 3 transitions represent less than $1.11\,\%$ (one-sigma limit) of the measured β-decay strength of ^{26}P.

Atomic mass excess $\Delta(^{26}P)$: The mass excess of ^{26}P was derived from the following relation:

$$\Delta(^{26}P) \;=\; \Delta(^{26}Si) + E^*(IAS) + \Delta E_c - \Delta_{nH} \qquad (3)$$

where $\Delta(^{26}Si)$ is the atomic mass excess of ^{26}Si. $E^*(IAS) = 13015\,(4)\,keV$ is the previously obtained excitation energy of the IAS in ^{26}Si and Δ_{nH} is the mass excess difference between a neutron and a hydrogen atom. ΔE_c is the Coulomb energy difference between the IAS of ^{26}Si and the ground state of ^{26}P. It can be deduced from the semi-empirical relation given in reference [40]:

$$\Delta E_c \;=\; 1440.8 * \left(\frac{\bar{Z}}{A^{\frac{1}{3}}}\right) \;-\; 1026.3 \qquad (4)$$

Taking $\bar{Z} = 14.5$ as a mean atomic number for the two $A = 26$ nuclei, the atomic mass excess of ^{26}P was deduced to be equal to $11114\,(90)\,keV$. This value is in agreement with the mass prediction from Audi *et al.* [41] of 10970(200) keV. It leads to a Q_{EC} value of $Q_{EC} = \Delta(^{26}P){-}\Delta(^{26}Si) = 18258\,(90)$ keV.

Search for other charged-particle emission modes: The one-proton separation energy of ^{26}P is given by the relation $S_p(^{26}P) = \Delta(H){+}\Delta(^{25}Si){-}\Delta(^{26}P)$, where $\Delta(H)$ and $\Delta(^{25}Si)$ are the

atomic mass excesses of hydrogen and ^{25}Si [41]. The deduced value $S_p(^{26}P) = 0\,(90)\,keV$ suggests that ^{26}P can hardly be a direct proton emitter since the available energy for such a disintegration would not exceed $100\,keV$.

In the same way, the relevance of β-delayed α emission can be discussed. Assuming that α particles would be emitted by the IAS of ^{26}Si, the corresponding Q_α value is given by the following relation:

$$Q_\alpha = E^*(IAS) + \Delta(^{26}Si) - \Delta(^{22}Mg) - \Delta(^{4}He) \quad (5)$$

Taking into account the atomic mass excesses given in reference [41] and the excitation energy of the IAS measured in this work, the available energy in such a β-delayed α decay would be equal to $3842\,(15)\,keV$. The α transitions towards the ground state and the first two excited states of ^{22}Mg are therefore energetically possible and would lead to three α groups at 3840, 2600 and $530\,keV$, the last two being followed by γ rays at 1250 and $2060\,keV$. No evidence for such γ lines was observed and the proton groups whose energy could match with an α decay to the ground state of ^{22}Mg (transitions 21 and 22 in table 5 and 6) were convincingly identified as ^{26}P β-delayed one- and two-proton transitions. In addition, these α transitions would be forbidden transitions. Hence, we conclude that β-delayed one- and two-proton emission are the only decay modes of the IAS in ^{26}Si.

The excitation energy and the β feeding of proton emitting states in ^{26}Si deduced from the present analysis are given in table 6. The summed feeding of ^{26}Si proton-unbound excited states is deduced to be equal to $39\,(2)\,\%$.

3.2.2 β-delayed γ decay

The γ-ray spectrum obtained during the ^{26}P setting is shown in figure 11. The six γ lines at $972\,(1.27\,(54)\,\%)$, $988\,(5.2\,(11)\,\%)$, $1796\,(52\,(11)\,\%)$, $1960\,(1.32\,(34)\,\%)$, $2046\,(1.44\,(40)\,\%)$ and $2342\,keV$ $(1.28\,(51)\,\%)$ are assigned to the β-delayed γ decay of ^{26}P according to reference [4]. A new γ ray at $1400.5\,(5)\,keV$ $(2.82\,(69)\,\%)$ was attributed to the deexcitation of the $4184\,keV$ excited state of ^{26}Si to the state at $2784\,keV$. The measured absolute intensities were combined with previously measured relative γ-ray intensities [4] to determine absolute β feedings. The values obtained are reported in table 7.

The β decay of the ground state of ^{26}Si is followed by two γ rays at 830 and $1622\,keV$. The two lines at 1341 and $2307\,keV$ are due to the summing of the $511\,keV$ γ rays (from the annihilation of the emitted positrons) with the intense γ rays at 830 and $1796\,keV$.

The β-delayed one-proton and two-proton decays towards excited states in ^{25}Al and ^{24}Mg give rise to the observation of the γ rays at $452, 493, 845, 945, 1612, 1790\,keV$ and $1369\,keV$. The absolute intensity of the $1790\,keV$ γ line, which forms a doublet with the γ line at $1796\,keV$, was deduced from the previous determination of the proton-group intensities to the related excited level in ^{25}Al. Some of these γ lines are also due to the presence of contaminating nuclei: ^{25}Si (see chapter 3.1), ^{24}Al (γ rays at 1073 and $1369\,keV$) and ^{23}Mg (γ ray at $440\,keV$). Background γ lines are also visible in the spectrum

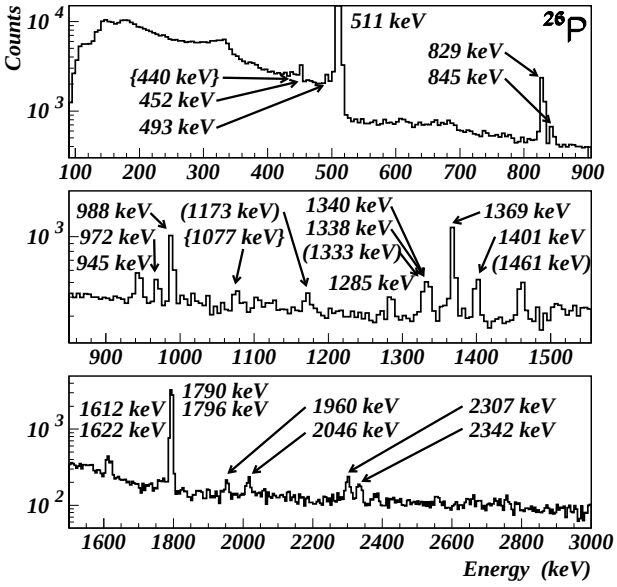

Fig. 11. γ-decay spectrum of ^{26}P: Background γ lines from ^{60}Co and ^{40}K are indicated within parenthesis. γ rays within brackets are due to the contaminating nuclei ^{23}Mg and ^{24}Al. All other γ lines are related to the β decay of ^{26}P, except the one at 1285 keV which could not be attributed.

at $1461\,keV$ (^{40}K), and at 1173 and $1333\,keV$ (^{60}Co). The γ ray at $1285\,keV$ could not be assigned.

According to tables 6 and 7, the summed feeding of ^{26}Si proton-unbound and proton-bound states is equal to $39\,(2)\,\%$ and $54\,(12)\,\%$, respectively. The spin of the ground state of the even-even nucleus ^{26}Si being equal to 0^+ [4], this state is not expected to be fed significantly by a second forbidden β decay of the 3^+ ground state of ^{26}P. The summed feeding of the excited states of ^{26}Si obtained in the present work is therefore equal to $93\,(13)\,\%$. Taking into account the large uncertainty, the result is in agreement with the expected value of $100\,\%$. However, unidentified weak proton groups or γ lines (see comparison to shell-model calculations below) may also contribute to the missing strength. In addition, it cannot be excluded that the β feeding of the $1796\,keV$ state was underestimated or that the γ decay of proton-bound states lying in the gap between 4184 and $5929\,keV$ of excitation energy (see decay scheme, figure 13) was not observed.

3.2.3 Measurement of the half-life of ^{26}P

The lifetime of ^{26}P was determined by means of a time correlation procedure. The applied technique is schematically shown in the inset of figure 12. It consists in measuring the time difference between the implantation of ^{26}P ions, identified by means of time-of-flight and energy-loss measurements, and the observation of β or β(2)p decay events.

Decay events that are correlated to the selected implantation event follow an exponential decay curve, whereas uncorrelated events due to the decay of contaminant ions, due to ^{26}P

C.M. proton energy (keV) from the decay to ^{25}Al states					^{26}Si proton emitting states	
$\frac{5}{2}_1^+$; 0	$\frac{1}{2}_1^+$; 452	$\frac{3}{2}_1^+$; 945	$\frac{7}{2}_1^+$; 1612	$\frac{5}{2}_2^+$; 1790	Energy	B.R. (%)
1 : 412 (2)					5929 (5)	17.96 (90)
2 : 778 (3)					6295 (6)	0.78 (7)
3 : 866 (2)					6384 (5)	1.71 (15)
4 : 1248 (2)					6765 (5)	1.51 (12)
8 : 1983 (2)					7501 (5)	2.39 (16)
	6 : 1638 (3)				7606 (6)	0.65 (6)
		5 : 1499 (2)			7962 (5)	0.99 (7)
13 : 2638 (18)					8156 (21)	0.11 (4)
14 : 2732 (4)		7 : 1798 (4)			8254 (5)	0.67 (7)
	12 : 2593(13)				8563 (17)	0.27 (6)
		16 : 2908(11)			9370 (15)	0.06 (5)
23 : 3920 (5)		17 : 2968 (5)	10 : 2288 (3)	9 : 2139 (4)	9433 (4)	3.54 (20)
	20 : 3766 (9)	19 : 3258 (4)			9725 (7)	0.59 (8)
26 : 4793 (3)		21 : 3817 (6)			10299 (6)	0.67 (7)
				18 : 3097 (6)	10405 (5)	0.31 (6)
	25 : 4719 (6)				10688 (9)	0.24 (4)
	27 : 4858 (4)				10827 (8)	0.44 (5)
33 : 7494 (4)	32 : 7039 (5)	31 : 6551 (4)	30 : 5893 (4)	29 : 5710 (3)	13015 (4)	3.12 (20)

C.M. two-proton energy (keV) from the decay to ^{24}Mg states		^{26}Si two-proton emitting states	
0_1^+; 0	2_1^+; 1369	Energy	B.R. (%)
28 : 5247 (3)	22 : 3879 (3)	13036 (4)	2.16 (24)

Table 6. Excitation energies and β feeding of the proton-unbound excited states of ^{26}Si. They are deduced from the data compiled in table 5. On the left-hand side, in the top row and in the row last but one, we give the final states on which the one- or two-proton emission ends. Then we indicate the peak numbers according to figure 10 and their center of mass proton energy. On the right-hand side, we use this information to determine the excitation energy of the emitting states in ^{26}Si as well as the β-decay branching ratio for the feeding of these states.

^{26}Si populated states	Excitation energy (keV)	B.R. (%)
2_1^+	1795.9 (2)	44 (12)
2_2^+	2783.5 (4)	3.3 (20)
(3_1^+)	3756 (2)	2.68 (68)
(4_1^+)	3842 (2)	1.68 (47)
2^+	4138 (1)	1.78 (75)
(3_2^+)	4184 (1)	2.91 (71)

Table 7. β-decay branching ratios towards proton-bound excited states of ^{26}Si.

daughter nuclei or due to ^{26}P implantations other than the one considered for the correlation are randomly distributed. The large time correlation window of $500\,ms$ enabled us to estimate accurately the contribution of uncorrelated events to the decay curve. The half-life of ^{26}P was measured to be $43.7\,(6)\,ms$, in agreement with the value given by Cable *et al.* [25] of $20^{+35}_{-15}\,ms$. We verified that, due to its relatively long half-life (2.21 s), the daughter decay of ^{26}Si does not alter the fit result.

3.2.4 β-decay scheme of ^{26}P

The proposed β-decay scheme of ^{26}P is shown in figure 13. The measured half-life as well as the Q_{EC} value obtained experimentally are reported. The distribution of ^{26}Si excited states appears to be well reproduced up to an energy of $7\,MeV$ by the shell-model calculations performed by Brown [37].

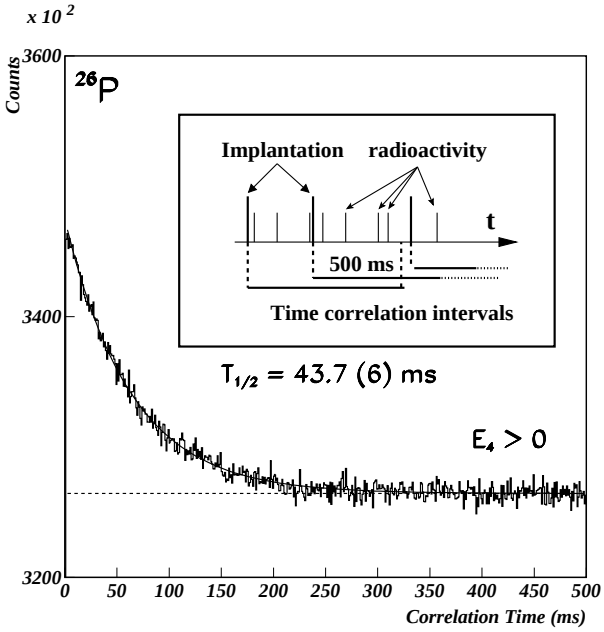

Fig. 12. Determination of the ^{26}P half-life by means of timing correlations between implantation and radioactivity events within a time window of $500\,ms$. The inset shows the correlation of each implantation event with each subsequent decay event within 500 ms.

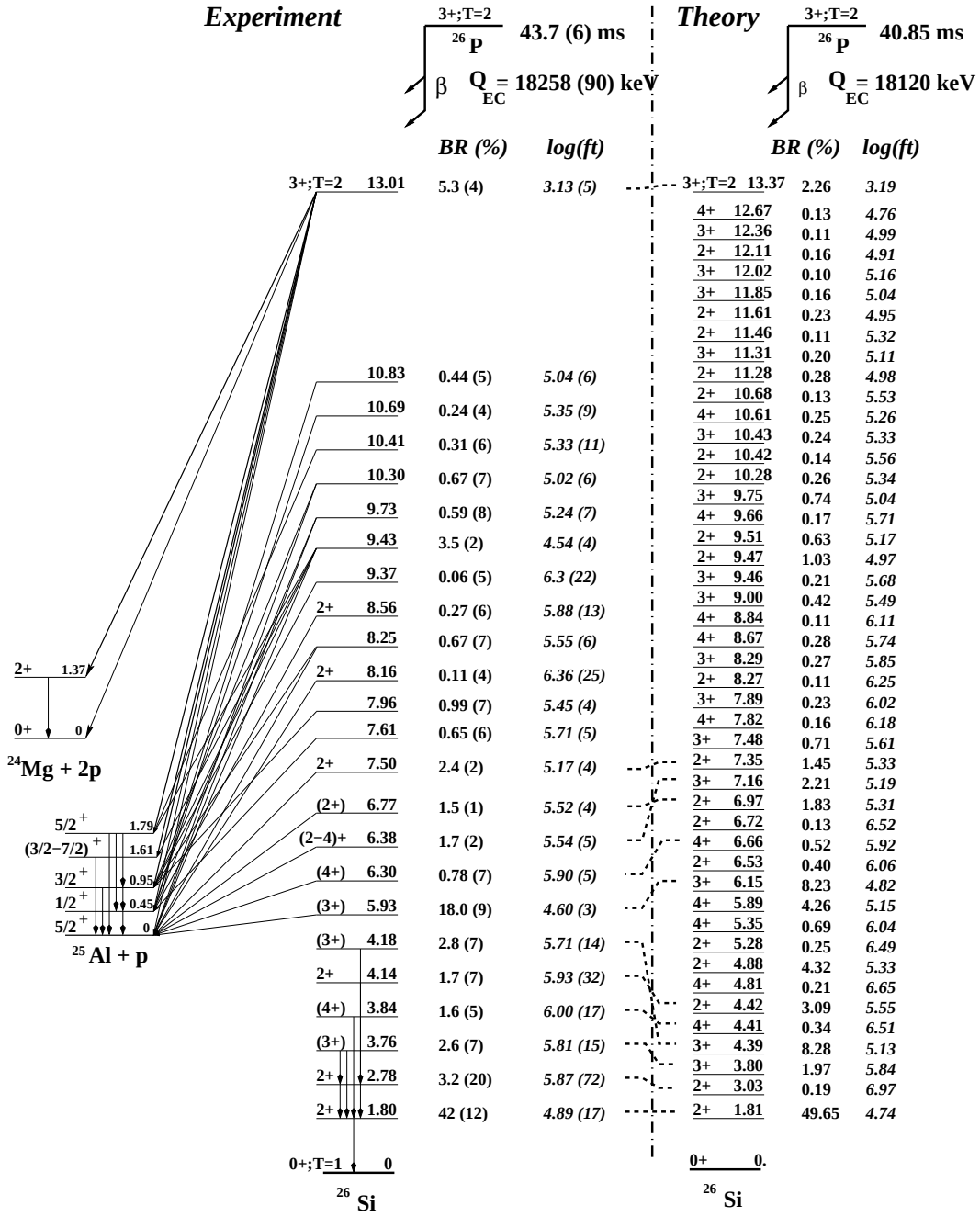

Fig. 13. ^{26}P β-decay scheme as deduced from the data presented in this work. The dotted lines tentatively connect experimentally determined levels to levels predicted by theory.

As shown in figure 14, the summed Gamow-Teller strength distribution is also well reproduced up to an excitation energy of more than $10\,MeV$. It can therefore be concluded that the quenching of the Gamow-Teller strength in the β decay of ^{26}P is about $60\,\%$, as it was the case for ^{25}Si.

At low excitation energy, the experimental Gamow-Teller strength distribution is in disagreement with the one derived theoretically between 4 and $6\,MeV$. The discrepancy can be due to the non-observation of populated excited states in this region, as it was mentioned before. The summed $B(GT)$ strength converges around $6\,MeV$ because of the high β-decay branching ratio towards the excited state at $5.93\,MeV$. Hence, the noticed discrepancy may simply originate from a different sharing of the β-decay strength between the two competing 3^+ excited states at 3.76 and $5.93\,MeV$.

Once again, the uncertainty of the β-decay branching ratios to low-energy excited states is too large (see table 8 below) to

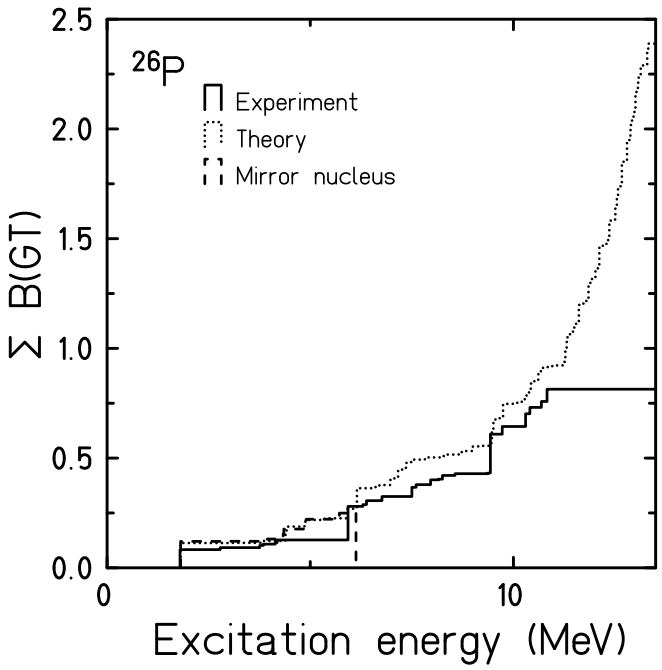

Fig. 14. Summed Gamow-Teller strength distribution in the decay of ^{26}P. The result of the present experiment (relative error of about 20%) is compared to shell-model calculations and to the B(GT) of the mirror decay of ^{26}Na assuming isospin symmetry.

derive precise values for the asymmetry parameter δ for the $(A=26, T=2)$ isospin multiplet (^{26}Na,^{26}Mg,^{26}Si,^{26}P).

3.3 Mirror asymmetry of mass A = 25, 26 nuclei

The mirror asymmetry parameter δ is usually determined for the ground-state transitions as well as for those feeding the low-lying excited states in the daughter nuclei. Higher-lying states are normally fed with smaller branching ratios which yields larger errors for the δ value. In addition, these states may decay by proton emission for the proton-rich partner which usually reduces the branching-ratio precission.

In the present experiment, however, the feeding of low-lying states and in turn also of the ground state (its branching ratio is determined as the difference between 100% and the observed branchings) is only poorly determined due to the large uncertainties of the γ-ray efficiency of our set-up. Nontheless, we give the asymmetry values derived from the present work for the mass $A = 25$ and $A = 26$ nuclei in table 8.

Experimentally, we reach the best precision for the highest-lying state in each mirror couple where the ft value for the proton-rich nucleus comes from a β-delayed proton branch. In both cases, a significant effect is observed. This result, however, is opposite in sign compared to the theoretical value for the mass A=25 couple. For the other mirror transitions, no clear statement can be made due to the large experimental errors for the decay of the proton-rich partner.

A	$E^*(MeV)$	$J_i^\pi;T_i$	$J_f^\pi;T_f$	theory [7]	present work
25	0.00	$\frac{5}{2}^+;\frac{3}{2}$	$\frac{5}{2}^+;\frac{1}{2}$	1.11	0(40)
	0.95		$\frac{3}{2}^+;\frac{1}{2}$	12.39	0(20)
	1.61		$\frac{7}{2}^+;\frac{1}{2}$	11.23	30(40)
	2.67		$\frac{5}{2}^+;\frac{1}{2}$	-5.58	48(11)
26	1.81	$3^+;2$	$2^+;1$		50(60)
	3.76		$3^+;1$		10(40)
	4.14		$2^+;1$		110(160)
	4.18		$3^+;1$		110(70)
	5.93		$3^+;1$		-24(11)

Table 8. Mirror asymmetries for the decay of ^{25}Si and ^{26}P and their mirror nuclei to low-lying states in the daughter nuclei. The excitation energies indicated in the second column are those of the β^+ daughter nuclei. Initial and final spin and isospin values are given in the following two columns. The experimental asymmetry results from our experimental values for the ft values of the β^+ decay and data from the literature [4]. The theoretical result is from ref. [7] where we took the INC+WS value as one example. The last transition for each mirror pair stems from the measurement of a β-delayed proton branch for the proton-rich nucleus.

4 Conclusion and perspectives

The β decay of the neutron-deficient nuclei ^{25}Si and ^{26}P was studied at the LISE3 facility at GANIL. 300 and 60 ions per second, respectively, were produced with contamination rates of less than $1\,\%$ and of about $13\,\%$. The decay scheme of the two nuclei was obtained, including for the first time the β-decay pattern towards proton-bound states. It allowed us to measure the asymmetry parameter δ for the mirror states of the mass A=25 and A=26 nuclei. Unfortunately, the poor precision in the determination of the corresponding branching ratios gave rise to large uncertainties for these δ values. Comparison to shell-model calculations based on the USD interaction and performed in the full sd shell by Brown [37] revealed two features: the reliability of such models when they are applied to mid-shell nuclei lying close to the proton drip-line, and the about $60\,\%$ quenching of the Gamow-Teller strength of the individual β transitions.

The following properties were derived from the spectroscopic study of these nuclei: i) The half-life of ^{26}P was measured to be equal to $43.7\,(6)\,ms$. ii) Its proton separation energy as well as the maximum available energy in its β decay were determined with a precision of $90\,keV$. iii) The β-delayed two-proton emission of ^{26}P towards the ground state and the first excited state of ^{24}Mg was observed. iv) More than thirty one-proton groups were identified, five of them being emitted from the isobaric analog state of ^{26}Si.

Compared to previous studies with a helium-jet technique, the use of projectile fragmentation in conjunction with a fragment separator has several advantages, which are that i) the detection of the arrival of an ion allow its identification and gives a start signal for half-life measurements, ii) very short half-lives can be studied since the separation time is short (order 1 microsecond), iii) the selection process is independent on chemistry.

Nonetheless, the spectroscopic studies presented here suffer from limitations that should be addressed in future experiments of the same type. Firstly, the implantation of ions inside a silicon detector gives rise to a high proton-detection efficiency, however, due to the energy deposit of β particles in the implantation detector, it is sometimes difficult to observe β-delayed protons with low intensity.

Secondly, concerning the γ-spectroscopy part, a high efficiency is required in order to identify low intensity γ rays, and a high precision is needed for the more intense transitions. A new detection set-up using segmented silicon detectors and four Germanium clovers has therefore been implemented and the decay properties of ^{21}Mg, ^{25}Si and their mirror nuclei were investigated recently at the GANIL facility [42]. This work should lead to the determination of accurate asymmetry parameters δ, which might help to understand the origin of isospin non-conserving forces in nuclei.

The author would like to thank B.A. Brown for providing up-to-date shell-model calculations and C. Volpe and N.A. Smirnova for stimulating discussions about the mirror asymmetry question. We would like to acknowledge the continous effort of the whole GANIL staff for ensuring a smooth running of the experiment. This work was supported in part by the Conseil Régional d'Aquitaine.

References

1. D.R. Tilley, H.R. Weller, and C.M. Cheves, Nucl. Phys. A 564, 1 (1993)
2. D.R. Tilley, H.R. Weller, C.M. Cheves, and R.M. Chasteler, Nucl. Phys. A 595, 1 (1995)
3. D.R. Tilley, C.M. Chevez, J.h. Kelley, S. Raman, and H.R. Weller, Nucl. Phys. A 636, 249 (1998)
4. P.M. Endt, Nucl. Phys. A 521, 1 (1990)
5. P.M. Endt, Nucl. Phys. A 633, 1 (1998)
6. B.H. Wildenthal, Prog. Part. Nucl. Phys. 11, 5 (1984)
7. N.A. Smirnova and C. Volpe, Nucl. Phys. A 714, 441 (2003)
8. I.S. Towner, Nucl. Phys. A 216, 589 (1973)
9. D.H. Wilkinson, Phys. Rev. Lett. 27, 1018 (1971)
10. D.H. Wilkinson and D.E. Alburger, Phys. Rev. Lett. 24, 1134 (1970)
11. L. Axelsson, J. Äystö, M.J.G. Borge, L.M. Fraile, H.O.U. Fynbo, A. Honkanen, P. Hornshøj, A. Jokinen, B. Jonson, P.O. Lipas, I. Martel, I. Mukha, T. Nilsson, G. Nyman, B. Petersen, K. Riisager, M.H. Smedberg, O. Tengblad, and the ISOLDE Collaboration, Nucl. Phys. A 634, 475 (1998)
12. S. Hatori, H. Miyatake, S. Morinobu, K. Katori, M. Fujiwara, I. Katayama, N. Ikeda, T. Fukuda, T. Shinosuka, and K. Ogawa, Nucl. Phys. A 549, 327 (1992)
13. K. Muto, E. Bender, and T. Oda, Phys. Rev. C 43, 1487 (1991)
14. J.-C. Thomas, PhD thesis, Centre d'Etudes Nucléaires de Bordeaux-Gradignan, Université Bordeaux I, France, 2002
15. F.C. Barker, Nucl. Phys. A 537, 147 (1992)
16. D.H. Wilkinson, Phys. Lett. 31 B, 447 (1970)
17. K. Kubodera, J. Delorme, and M. Rho, Phys. Rev. Lett. 38, 321 (1977)
18. D.H. Wilkinson, Eur. Phys. J. A 7, 307 (2000)
19. B.A. Brown and B.H. Wildenthal, At. Data Nucl. Data Tables 33, 347 (1985)
20. W.T. Chou, E.K. Warburton, and B.A. Brown, Phys. Rev. C 47, 163 (1993)
21. B.H. Wildenthal, M.S. Curtin, and B.A. Brown, Phys. Rev. C 28, 1343 (1983)
22. G. Martínez-Pinedo and A. Poves, Phys. Rev. C 53, R2602 (1996)
23. I.S. Towner and F.C. Khanna, Nucl. Phys. A 399, 334 (1983)
24. R.G. Sextro, R.A. Gough, and J. Cerny, Phys. Rev. C 8, 258 (1973)
25. M.D. Cable, J. Honkanen, E.C. Schloemer, M. Ahmed, J.E. Reiff, Z.Y. Zhou, and J. Cerny, Phys. Rev. C 30, 1276 (1984)
26. J.D. Robertson, D.M. Moltz, T.F. Lang, J.E. Reiff, and J. Cerny, Phys. Rev. C 47, 1455 (1993)
27. R. Barton, R. McPherson, R.E. Bell, W.R. Frisken, W.T. Link, and R.B. Moore, Can. J. Phys. 41, 2007 (1963)
28. B.D. Anderson, T. Chittrakarn, A.R. Baldwin, C. Lebo, R. Madey, D.M. Manley, M. Mostajabodda'vati, J.M. Watson, and W.M. Zhang, Phys. Rev. C 43, 50 (1991)
29. P.L. Reeder, A.M. Poskanzer, R.A. Esterlund, and R. McPherson, Phys. Rev. 147, 781 (1966)
30. M.D. Cable, J. Honkanen, R.F. Parry, S.H. Zhou, Z.Y. Zhou, and J. Cerny, Phys. Lett. 123B, 25 (1983)
31. L. Achouri, J. Äystö, R. Béraud, B. Blank, G. Canchel, S. Czajkowski, P. Dendooven, A. Ensallem, J. Giovinazzo, N. Guillet, J. Honkanen, A. Jokinen, A. Laird, M. Lewitowicz, C. Longour, F. de Oliveira Santos, M. Stanoiu, and J.-C. Thomas, in preparation
32. G. Canchel, L. Achouri, J. Äystö, R. Béraud, B. Blank, E. Chabanat, S. Czajkowski, P. Dendooven, A. Ensallem, J. Giovinazzo, J. Honkanen, A. Jokinen, A. Laird, M. Lewitowicz, C. Longour, F. de Oliveira Santos, M. Stanoiu, and J.-C. Thomas, Eur. Phys. J. A 12, 377 (2001)
33. A. Joubert, E. Baron, C. Grunberg, J.D. Larson, W. Mittig, and F. Ripouteau , Proc. Second Conference of the IEEE Particle Accelerator, San Francisco, May 1991, vol. 1, p. 594.
34. CERN web page at http://wwwinfo.cern.ch/asd/geant/
35. M.-J. Lopez-Jiménez, PhD thesis, Grand Accélérateur National d'Ions Lourds, Université de Caen, France, 2000
36. K. Debertin and R.G. Helmer, in *Gamma and X-ray spectrometry with semiconductor detectors*, edited by North-Holland, Elsevier Science Publishers B.V., Amsterdam, p 78. (1988)
37. B.A. Brown, private communication
38. A. Echegoyan, W.M.D. McRae, and B.A. Brown, MSU-NSCL Report No. 524 (1985)
39. Z.Y. Zhou, E.C. Schloemer, M.D. Cable, and M. Ahmed, Phys. Rev. C 31, 1941 (1985)
40. M.S. Antony, J. Britz, and A. Pape, At. Data Nucl. Data Tables 34, 279 (1986)
41. G. Audi, O. Bersillon, J. Blachot, and A.H. Wapstra, Nucl. Phys. A 729, 3 (2003)
42. J. Giovinazzo *et al.*, work in progress